11920 *Biochemistry* **2009,** *48,* 11920–11928
DOI: 10.1021/bi9016999

BIOCHEMISTRY
including biophysical chemistry & molecular biology
Article

Asp157 Is Required for the Function of PsbO, the Photosystem II Manganese Stabilizing Protein†

Hana Popelkova,*,‡ Alan Commet,‡ and Charles F. Yocum‡,§

‡*Department of Molecular, Cellular and Developmental Biology and* §*Department of Chemistry, The University of Michigan, Ann Arbor, Michigan 48109-1048*

Received September 30, 2009; Revised Manuscript Received November 6, 2009

ABSTRACT: PsbO, the photosystem II manganese stabilizing protein, contains an aspartate residue [Asp157 (spinach numbering)], which is highly conserved in eukaryotic and prokaryotic PsbOs. The homology model of the PSII-bound conformation of spinach PsbO presented here positions Asp157 in the large flexible loop of the protein. We have characterized site-directed mutants (D157N, D157E, and D157K) of spinach PsbO that were rebound to PsbO-depleted PSII to probe the role of Asp157. Structural data revealed that PsbO Asp157 mutants exhibit near-wild-type solution structure at 25 °C, but functional analyses of the mutants showed that these are the first genetically modified PsbO proteins from spinach that combine wild-type PSII binding behavior with significantly impaired O_2 evolution activity; all of the mutants reconstituted ~30% of control O_2 evolution activity. PsbO Asp157 has been proposed to be a part of a putative H_2O/H^+ channel that links the active site of the oxygen-evolving complex with the lumen [De Las Rivas, J., and Barber, J. (2004) *Photosynth. Res. 81*, 329−343]. Unsuccessful attempts to use chemical rescue to enhance the activity restored by Asp157 mutants could indicate that this residue is not involved in a proton transfer network. It is shown, however, that these mutants are deficient in restoring efficient Cl^- retention by PSII.

Production of atmospheric O_2 from H_2O by oxygenic photosynthesis takes place in the oxygen-evolving complex (OEC)[1] of Photosystem II (PSII), which consists of three inorganic cofactors (Mn, Ca^{2+}, and Cl^-), and both intrinsic and extrinsic proteins. High rates of O_2 evolution activity are assured by the presence of the largest extrinsic PSII subunit called PsbO, or the manganese stabilizing protein, found in all prokaryotic and eukaryotic photosynthetic organisms (*1*). The amino acid sequence of PsbO contains ~250 amino acids and has a large number of charged residues, many of which are highly conserved (*2*, *3*). Anomalous solution behavior identifies PsbO as a natively unfolded polypeptide (*4*); it possesses a low pI (5.2), produces exaggerated size estimates in SDS−PAGE and gel filtration experiments (33 and 40 kDa, respectively) as compared to its actual molecular mass (26.5 kDa), is thermostable, and has a high content of unordered elements in its secondary structure (*3*, *5*). The current understanding of the solution structure of spinach PsbO comes from biochemical and spectroscopic studies, because the natively unfolded nature of PsbO causes difficulties in crystallization of the protein. The only crystallographic model of PsbO that is currently available is that of cyanobacterial PsbO bound to PSII (*6*−*9*). As the solution and the PSII-bound conformations of PsbO differ (*10*) and PsbOs from prokaryotes and eukaryotes are not identical (*2*, *3*), a detailed structure of PsbO is not available. In solution, PsbO has a prolate ellipsoid shape (*11*, *12*), the C- and N-termini are in the proximity of one another, and the C-terminus is buried in a hydrophobic environment; a single S−S bond is found in all PsbOs near the N-terminus (*3*, *13*−*17*).

Overexpression of spinach and *Arabidopsis* PsbOs in *Escherichia coli* and successful reconstitution of PsbO-depleted PSII membranes with the recombinant proteins (*18*, *19*) provided a method for functional and structural analyses of PsbO using site-directed mutagenesis. A number of such mutants from spinach were produced that exhibit a wide range of effects on PSII binding, O_2 evolution activity, and PsbO structure. For example, removal of the disulfide bond (the C28A/C51A mutation) preserves the PSII binding, activity restoration, and thermostability of the protein but disrupts its solution structure (*19*, *20*). Retention of PsbO's 84-amino acid signal peptide has an effect similar to that of the C28A/C51A mutation on the protein's binding, activity, and solution structure and in addition causes nonspecific binding of the protein to PSII (*21*). Deletion of residues at the C-terminus (E246stop, L245stop, and Q244stop) alters the solution structure of PsbO so that the protein cannot bind efficiently and assemble into PSII binding sites (*22*, *23*). The V235A mutation weakens binding of PsbO to one of two sites and induces temperature-sensitive assembly of the protein into PSII (*24*, *25*). Deletion of some N-terminal amino acids

†This research was supported by grants to H.P. and C.F.Y. from the National Science Foundation (MCB- 0716541).

*To whom correspondence should be addressed: Department of Molecular, Cellular and Developmental Biology, The University of Michigan, Ann Arbor, MI 48109-1048. Telephone: (734) 764-9543. Fax: (734) 647-0884. E-mail: popelka@umich.edu.

[1]Abbreviations: BSA, bovine serum albumin; CCCP, carbonylcyanide *m*-chlorophenyl hydrazone; CD, circular dichroism; DCBQ, 2,6-dichloro-1,4-benzoquinone; HEPES, 4-(2-hydroxyethyl)-1-piperazineethanesulfonic acid; IPTG, isopropyl β-D-thiogalactopyranoside; MES, 2-(*N*-morpholino)ethanesulfonic acid; MRE, mean residue ellipticity; PDB, Protein Data Bank; PsbO, manganese-stabilizing protein; OEC, oxygen-evolving complex; PAGE, polyacrylamide gel electrophoresis; PS, Photosystem; SDS, sodium dodecyl sulfate; SW-PSII, NaCl-washed Photosystem II membranes depleted of 23 and 17 kDa extrinsic proteins; Tris, tris(hydroxymethyl)aminomethane; UW-PSII, urea NaCl-washed Photosystem II membranes depleted of PsbO, PsbP, and PsbQ (33, 23, and 17 kDa, respectively) extrinsic proteins.

 Published on Web 11/07/2009 © 2009 American Chemical Society

(ΔG3M, ΔR5M, and ΔL6M) has no effect on the PSII binding or O_2 evolution activity of PsbO, but the mutants bind nonspecifically to PSII (*21*, *26*). Further deletions at the PsbO N-terminus, up to 14 residues (ΔT7M, ΔE10M, ΔS13M, and ΔK14M mutations), eliminate specific binding of one of two PsbO copies to PSII and in some cases also cause nonspecific binding of PsbO to PSII. These mutants exhibit only 40−50% of the control activity of SW PSII preparations (*26*, *27*). Truncations of 15 or 18 N-terminal residues (ΔT15M and ΔE18M mutations) result in very weak binding of one PsbO subunit, and a further decrease in activity to ~10% of the control (*26*, *27*). Three Arg mutations in the large flexible loop of PsbO (R151G, R151D, and R161G) decrease the PSII binding affinity, lower O_2 evolution activity to 20−40% of the control, and weaken retention of Cl^- by PSII (*28*). Replacement of aromatic residues W241 and Y242 with Phe significantly impairs binding of PsbO to PSII and restores only ~30% of the control activity (*17*).

In this paper, we report data on the structure and function of three mutations of Asp157, a highly conserved residue in all PsbOs sequenced to date. While structural characterization showed that these mutants (D157N, D157E, and D157K) retain near-wild-type solution structure at 25 °C, functional analyses revealed that these are the first mutant PsbOs from spinach that exhibit wild-type PSII binding along with significantly lowered O_2 evolution activity (~30% of the control). These results indicate an important role of Asp157 for PsbO function in PSII. It has already been proposed that PsbO Asp157 is a part of a H_2O/H^+ channel that links the OEC active site with the lumen (*6*, *29*). Results of experiments that attempt rescue proton transfer using a proton acceptor in UW-PSII reconstituted with Asp mutants are described, along with results of experiments that show that Asp157 is required for efficient Cl^- retention by PSII.

MATERIALS AND METHODS

PsbO Mutagenesis. Site-directed mutants of the *psbO* gene from spinach that include replacements of Asp157 with Asn, Glu, or Lys in the TOPO vector (Invitrogen) were produced using the Stratagene technique (Stratagene, La Jolla, CA) as described in ref *28*, except that the following synthetic oligonucleotides for mutagenesis were used: D157N sense, 5′-CCTCGTTCCTTAACCCAAAGGGCCGAGG-3′; D157N antisense, 5′-CCTCGGCCCTTTGGGTTAAGGAACGAGG-3′; D157K sense, 5′-CCTCGTTCCTTAAGCCAAAGGGCCGAGG-3′; D157K antisense, 5′-CCTCGGCCCTTTGGCTTAAGGAACGAGG-3′; D157E sense, 5′-CCTCGTTCCTTGAGCCAAAGGGCCGAG-3′; and D157E antisense, 5′-CTCGGCCCTTTGGCTCAAGGAACGAGG-3′. After verification of the correct mutations and an absence of errors in the *psbO* sequence by DNA sequencing, the mutated *psbO*-TOPO constructs were transformed into BL21(DE3)pLysS *E. coli* cells. The correct reading frame (starting with EGGKR) during protein translation and subsequent processing in *E. coli* was verified by N-terminal sequencing of the mutant proteins.

Overexpression and Purification of Recombinant PsbOs. The D157N, D157E, and D157K PsbO proteins were produced by overexpression of the *psbO*-TOPO construct at 37 °C and 130 rpm agitation for 3.5 h in LB medium containing 50 μg/mL ampicillin. Overexpression was induced with 25 μM IPTG. After isolation of inclusion bodies (*19*), the mutated proteins were purified in two steps [gradient elution (50 to 250 mM NaCl) followed by step elution (30 mM, 150 mM, 500 mM, and 1 M NaCl), all in the presence of 3 M urea and 5% betaine], as described in ref *28*. PsbO eluted at ~150 mM NaCl. After dialysis in refolding buffer [100 mM Tris and 10 mM NaCl (pH 8)] and pH-adjustment buffer [50 mM MES and 10 mM NaCl (pH 6)], sucrose was added to a final concentration of 0.4 M and the pure, soluble proteins were stored at −70 °C.

Reconstitution of PSII with Recombinant PsbO and Activity Assays. Intact PSII (containing the 33, 23, and 17 kDa extrinsic proteins), SW-PSII, and UW-PSII membranes were prepared from spinach and stored as described in refs *21* and *28*. UW-PSII membranes were reconstituted with wild-type (WT) or mutant PsbOs for 1 h at room temperature in a reconstitution buffer (buffer A) containing 37 mM MES (pH 6), 100 μg/mL BSA, 0.3 M sucrose, 2% betaine (w/v), and various concentrations of Ca^{2+} and Cl^- depending on the experiment. The Chl concentration in the reconstitution mixtures was 200 μg/mL. Oxygen evolution assays were performed in assay buffer (buffer B) containing 0.4 M sucrose, 50 mM MES (pH 6), 600 μM DCBQ (used as the electron acceptor), 100 μg/mL BSA, and concentrations of Ca^{2+} and Cl^- determined by the experiment (see below); the assay mixtures contained 15 μg of Chl.

The O_2 evolution rate assayed under saturating light conditions for 1 min monitored PSII turnover, while the O_2 evolution yield was assayed at 80% light saturation for 4 min to determine the long-term stability of the reconstituted system. Rebinding of recombinant protein to UW-PSII was assessed by integration of Coomassie-stained PsbO bands via SDS−PAGE as described in ref *28*. The data in Figure 2 are averages of three independent activity assays and four SDS−PAGE gels.

For standard activity assays (Figure 2), the reconstitution buffer (A) contained 10 mM Ca^{2+} and 110 mM Cl^- and the assay buffer (B) included 20 mM Ca^{2+} and 100 mM Cl^-. In the experiments to determine the Cl^- K_M, buffer A contained 10 mM Ca^{2+} and 17.5 mM Cl^-, while for the experiment to determine the Ca^{2+} K_M, buffer A included 100 mM Cl^-; Ca^{2+} was omitted from the reconstitution mixture. In the O_2 evolution assays conducted with varying Cl^- concentrations, the Ca^{2+} concentration was constant (20 mM) and Cl^- concentrations ranged between 700 μM and 50.7 mM. The assays with varying Ca^{2+} concentrations were conducted at a constant Cl^- concentration (100 mM); Ca^{2+} concentrations ranged from 4 μM to 9.5 mM. O_2 evolution activity as a function of increasing Ca^{2+} or Cl^- concentrations was measured three times for each mutant PsbO; K_M values were determined from the averaged data points. The pH optimum was determined for PsbO WT and Asp157 mutants using activity assays over a pH range from 5 to 7.5. UW-PSII was reconstituted with PsbO in buffer A that contained 10 mM Ca^{2+} and 40 mM Cl^- (to prevent a high Cl^- concentration in activity assays). For activity assays, buffer B contained 5.5 mM Ca^{2+} and 12, 25, 50, or 100 mM Cl^-. MES was used in buffer B for the pH range from 5 to 6.5, while HEPES was used for pH 7 and 7.5. The data in Figure 5 are averages of two or three independent experiments for each concentration of Cl^- in buffer B. The reagents (CCCP, imidazole, and acetate) used to attempt the chemical rescue of possible disruptions to a proton transfer network were added to the standard assay buffer described above, prior to illumination.

UV and CD Spectroscopy and Size-Exclusion Chromatography. The recombinant PsbO proteins were dialyzed against 10 mM KH_2PO_4 buffer (pH 6) and used for UV and CD spectroscopy at 25 °C as described in refs *21* and *28*. The mutant

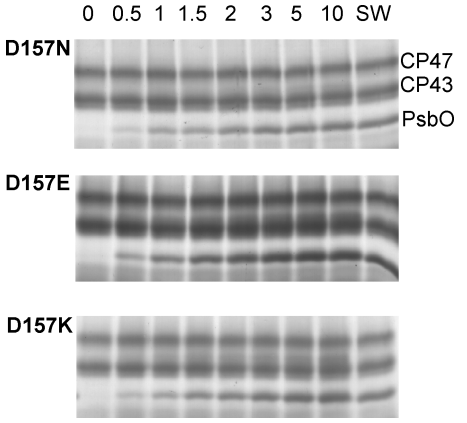

FIGURE 1: Coomassie blue-stained SDS−PAGE gels of UW-PSII membranes reconstituted with Asp157 mutants of PsbO. The moles of PsbO per mole of PSII used for reconstitution are indicated at the top of the lanes; SW indicates control SW-PSII membranes, and 70 μg of Chl was loaded in each lane. The identity of Coomassie blue-stained bands is indicated at the right. Gels were analyzed by densitometry, and Coomassie staining of CP47 was used as an internal standard to control for slight differences in protein loading.

proteins in 10 mM KH_2PO_4 (pH 6) and 0.4 M sucrose were used for gel filtration experiments as described in ref *21*. The molecular mass values represent the average of three or four runs for each mutant with a standard deviation of less than 2%.

Alignment of PsbO Sequences. Amino acid sequence alignments were generated in the BioEdit Sequence Alignment Editor (1997−2004 Tom Hall Isis Pharmaceuticals, Inc.; *30*) using the PsbO sequences available at the NCBI (http://www.ncbi.nlm.nih.gov/).

Homology Modeling. The homology model of the PSII-bound conformation of spinach PsbO was constructed using the DeepView/Swiss-PDBViewer program (http://spdbv.vital-it.ch/) and the SWISS-MODEL server (*31*−*33*). The crystal structure of the PSII-bound conformation of PsbO from *Thermosynechococcus elongatus* [PDB entry 2AXT (*8*)] was used as a template. The amino acid sequences of spinach and cyanobacterial PsbO were aligned before the modeled (spinach) PsbO sequence was fitted onto the template (cyanobacterial) PsbO sequence. Alignment required insertion of a gap at the N-terminus of the cyanobacterial sequence and in the middle of the spinach sequence (see refs *2* and *27*). The model generated by the SWISS-MODEL server was adjusted for amino acid clashes in the DeepView/Swiss-PDBViewer program.

RESULTS

PSII Binding and O_2 Evolution Activity of Asp157 Mutants. Reconstitution of UW-PSII preparations with the D157N, D157E, or D157K PsbO mutants was conducted to determine the effect of the mutations on the functional integrity of reconstituted samples. Figure 1 shows the Coomassie blue-stained SDS−PAGE gels of UW-PSII reconstituted with increasing concentrations of each of the PsbO mutants; the numbers above the lanes give the moles of PsbO per mole of PSII reaction center. A SW-PSII sample diluted in reconstitution buffer is the control for 100% PsbO binding. The mutant protein's migration pattern is similar to that of the native wild-type protein (Figure 1). Densitometric evaluation of the Coomassie-stained PsbO bands on the SDS−PAGE gels is shown in Figure 2 as a binding curve (●) for each mutant. Figure 2 also presents data on

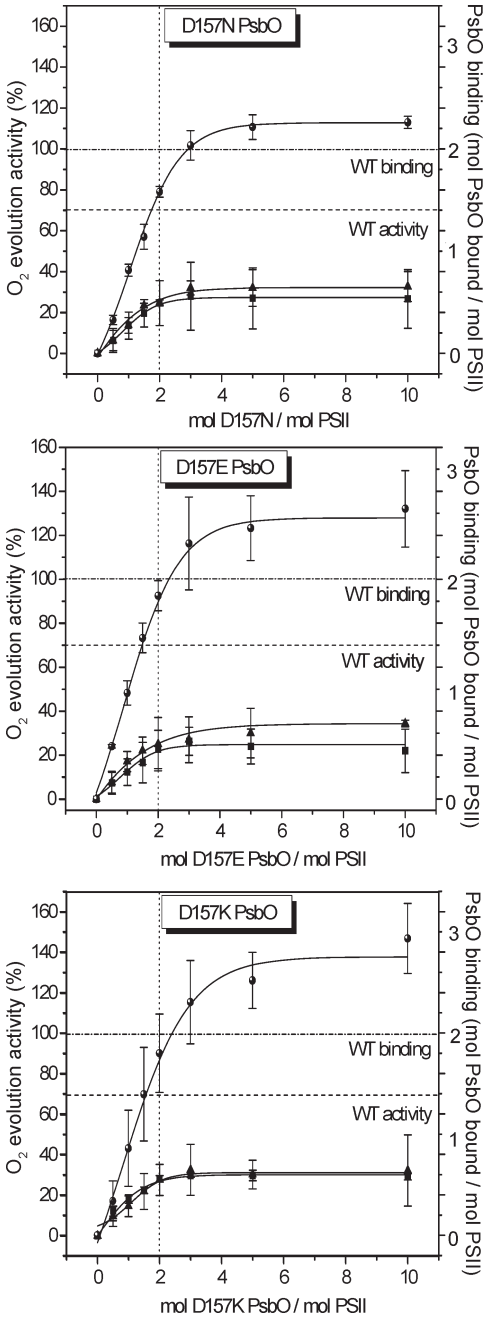

FIGURE 2: Binding and recovery of O_2 evolution activity by UW-PSII membranes reconstituted with Asp mutants of PsbO: (●) binding curves (analysis of SDS−PAGE gels in Figure 1), (■) O_2 evolution rate, and (▲) O_2 evolution yield plotted as a function of moles of PsbO per mole of PSII added to the reconstitution mixtures. Residual activity of UW-PSII was subtracted from the activities of reconstituted samples; 100% corresponds to the activity of SW-PSII samples [250−400 μmol of O_2 (mg of Chl)$^{-1}$ h^{-1}]. Points are the averages, and vertical bars at each point give the standard deviation. Dotted, dashed, and dotted−dashed lines show saturation of the wild-type PsbO activity and binding of 2 mol of PsbO/mol of PSII.

restoration of O_2 evolution rates (■) and yields (▲). The binding curves show that all of the mutants bind at slightly lower stoichiometries than the wild type when 2 mol of PsbO/mol PSII is present in the reconstitution mixture. Between 1.6 and 1.8 mol of a mutant protein was bound to UW-PSII with 2 mol of PsbO/mol of PSII present in the reconstitution mixture, as compared to 2 mol of wild type rebound to UW-PSII (indicated by dotted and dashed−dotted lines) under the same conditions, which was used

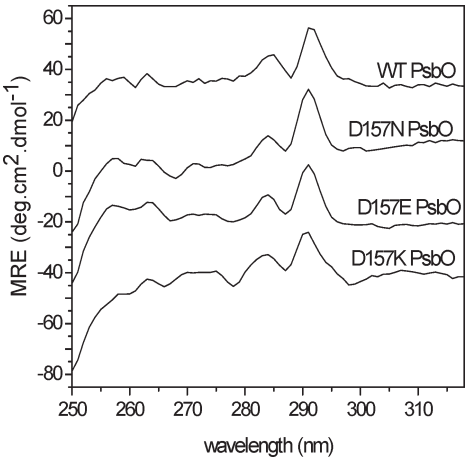

FIGURE 3: Near-UV CD spectra of wild-type PsbO and Asp157 mutants. The solvent was 10 mM KH_2PO_4 buffer (pH 6) at 25 °C. MRE was calculated on the basis of the protein concentration. The experimental conditions were as follows: path length, 1 cm; sample volume, 1 mL; time constant, 1 s; bandwidth, 1 nm.

as a control in these experiments. When the protein concentration in the reconstitution mixture was increased above 2 mol of PsbO/mol of PSII, binding of the mutant proteins to UW-PSII gradually saturated and even exceeded binding of WT PsbO; between 2.0 and 2.5 mol of the Asp mutants was bound to UW-PSII when 3 mol of PsbO/mol of PSII was present in the reconstitution mixture, and between 2.2 and 2.8 mol of mutant PsbOs was bound to UW-PSII when 5 mol of PsbO/mol of PSII was used for reconstitution. These data indicate that, in addition to binding to the specific PSII sites, the D157N, D157E, and D157K mutants exhibit modest levels of nonspecific binding to PSII. Despite high-affinity binding, PsbO Asp mutants reconstituted ~30% of the control (SW-PSII) activity at 3−10 mol of PsbO/mol of PSII added to the reconstitution mixture, as compared to the result with the wild-type protein, for which reconstitutions of ~70% of the control activity at 2 mol of PsbO/mol of PSII (indicated by dotted and dashed lines) are obtained. Neither mutant was cold-sensitive (data not shown), a phenomenon that was previously observed with two PsbO mutants, V235A and ΔL6MW241F (*17*, *24*).

Solution Structure of Asp Mutants at 25 °C. Although functional characterization of PsbO Asp mutants (Figures 1 and 2) showed that the replacement of Asp157 with Asn, Glu, or Lys compromises PsbO activity, the spectroscopic and biochemical data presented here indicate that the solution structures of Asp mutants at 25 °C were similar to that of WT PsbO. The tertiary structure of PsbO in solution can be monitored by near-UV CD spectroscopy that provides information about the microenvironment of aromatic amino acids (Tyr, Trp, and Phe) that are buried in hydrophobic domains of the protein. Changes in protein tertiary structure that affect the microenvironment of these residues alter their corresponding characteristic wavelengths and amplitudes in near-UV CD spectra (*34*). The near-UV CD spectrum of wild-type PsbO has the largest peak at 291−293 nm that is assigned to the single Trp in the PsbO sequence (*2*, *3*, *17*). Several studies provide evidence that this residue is buried in a hydrophobic environment (*8*, *15*, *17*). Solvent-inaccessible Tyr and Phe residues exhibit less pronounced signals in the near-UV CD spectrum of PsbO; the peak at 285−287 nm comes from Tyr, while the weak signals at 258 and 264 nm are assigned to Phe (*2*, *3*, *17*) (see Figure 3). As Figure 3 shows, the near-UV CD

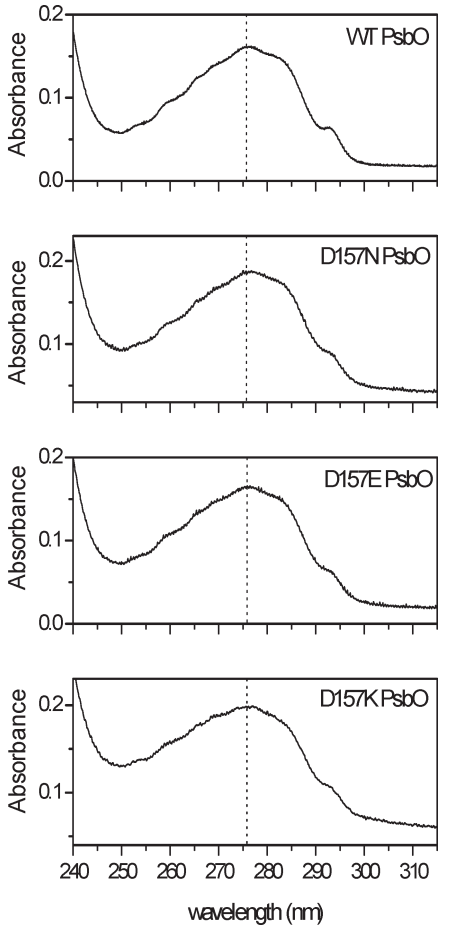

FIGURE 4: UV absorption spectra of the wild-type PsbO and Asp157 mutants. The proteins were in 10 mM KH_2PO_4 buffer (pH 6) at 25 °C. The spectra were normalized to a final concentration of 10 μM. The experimental conditions were as follows: path length, 1 cm; sample volume, 1 mL; scan width, 320−240 nm.

spectra for WT and Asp PsbO mutants are very similar, except for the D157K spectrum that exhibits a slight increase in MRE around 270 nm, which might be due to a trace of DNA contamination. The subtle modification of the Phe peak at 258 nm in the D157K spectrum is difficult to interpret, because 13 Phe residues in eukaryotic PsbO are distributed throughout the amino acid sequence and an alteration at 258 nm was not observed in the near-UV CD spectra of D157N and D157E, mutants that exhibit the same functional defects as D157K. All Asp mutants had nearly identical tertiary structure when monitored by UV absorption spectroscopy (Figure 4). The absorbance features in the UV spectrum of WT PsbO include a characteristic shoulder at 293 nm assigned to Trp, an absorption maximum at 276 nm due to Tyr and Trp, and two Phe peaks at 259 and 266 nm (*17*, *34*) (Figure 4). The UV spectra of Asp mutants resemble the spectrum of the wild type, except that the Trp shoulder at 293 nm in the mutants is slightly less pronounced (Figure 4). The secondary structure elements in a protein can be calculated from its far-UV CD spectra. The second, third, and fourth columns in Table 1 present the secondary structure content estimated from the far-UV CD spectra of WT and Asp157 mutants of PsbO that were measured at 25 °C. The fifth column in Table 1 presents apparent molecular masses for all PsbO variants that were determined using size-exclusion chromatography. These data demonstrate that the

Table 1: Secondary Structure and Overall Molecular Size of Wild-Type and Asp Mutants of PsbO in Solution at 25 °C[a]

protein	α-helix[b]	β-sheet[b]	turn + unstructured[b]	size (kDa)
WT PsbO	3−4[c]	36−41[c]	56−60[c]	35
D157N PsbO	3	35	61	35
D157E PsbO	3	37	59	36
D157K PsbO	3	41	55	35

[a]Secondary structure was predicted on the basis of analysis of far-UV CD spectra, and molecular size was determined using a calibrated gel filtration column. [b]Prediction of secondary structures was calculated on the basis of basis sets of 42 or 48 proteins of which five proteins are denatured (apo-cytochrome *c* at 5 and 90 °C, ribonuclease at 20 °C, and staphylococcal nuclease at 6 and 70 °C). Numbers are averages of results obtained from the basis sets and from both CONTIN/LL and CDSSTR methods (see ref *51*). [c]Data from refs *17* and *21*.

mutants exhibited estimated secondary structures and apparent molecular masses very similar to those of WT PsbO.

Proton Transfer and Ca^{2+} and Cl^- Retention in UW-PSII Reconstituted with Asp Mutants. It has been proposed that PsbO Asp157 is a component of a putative H^+ channel linking the OEC with the thylakoid lumen (*29*). In theory, if mutagenic removal of D157 from PsbO impairs delivery of protons to the channel through this acidic residue, then proton transfer might be restored by addition of a proton acceptor to assay mixtures. Both SW-PSII and UW-PSII reconstituted with Asp mutants were tested for activity in the presence of varying concentrations of imidazole, sodium acetate, or carbonyl cyanide *m*-chlorophenyl hydrazone (CCCP), which have been previously used as proton acceptors (*35*−*37*); SW-PSII was used as the control sample to monitor a potential inhibitory effect of any of the acceptors. The activity assays showed that imidazole and CCCP, when added to the assay buffer, inhibited SW-PSII even at very low concentrations [0.6 mM and 0.25 μM, respectively (data not shown)]. Sodium acetate did not inhibit the control sample at a concentration of 50 mM, but the reconstituted sample mixed with this concentration of sodium acetate did not exhibit any enhancement in O_2 evolution activity (data not shown). This result would suggest that low O_2 evolution activity in Asp mutants (Figure 2) might not be due to mutagenic disruption of a proton transfer network or alternatively that the compounds used here cannot be used to restore proton transfer in PSII.

Failure to obtain increased rates of electron transfer with proton acceptors prompted additional experiments for examination of the origin of the lower activities reconstituted by the PsbO Asp157 mutants. The K_M values for Ca^{2+} and Cl^- were determined, and the results of these experiments are summarized in Table 2. While little if any effect is seen for Ca^{2+}, increases in the Cl^- K_M values are observed with all three of the Asp mutants. This result is similar to that reported earlier for PsbO mutants carrying N-terminal truncations that limit rebinding to PSII to one copy of the protein (*26*, *27*).

A decrease in the level of retention of Cl^- by Asp157 mutants, as compared to wild type, is also evident from the results of the experiments exploring the pH optimum of all four PsbO variants at 12, 25, 50, and 100 mM Cl^- (Figure 5). At 12 mM Cl^-, WT PsbO has an activity maximum at pH 6.5, while the Asp157 mutants all have an optimum at pH 6. Increasing the Cl^- concentration in the assay buffer to 25 mM shifts the wild-type pH optimum to 6.5−7, while all of the mutants exhibit pH optima at 6−6.5. Furthermore, O_2 evolution activity for

Table 2: Ca^{2+} and Cl^- K_M Values for SW-PSII Preparations and UW-PSII Membranes Reconstituted with WT PsbO and Asp Mutants (10 mol of MSP/mol of PSII)[a]

	K_M (mM)	
	Cl^-	Ca^{2+}
SW-PSII	0.9[b]	0.15[b]
UW-PSII and WT PsbO	1.0[b]	0.09[b]
UW-PSII and D157N PsbO	1.6	0.13
UW-PSII and D157E PsbO	1.5	0.10
UW-PSII and D157K PsbO	1.6	0.11

[a]The K_M values were determined from Ca^{2+} and Cl^- titration curves using assay conditions described in Materials and Methods. [b]Data from ref *48*.

WT PsbO significantly increases with enhancement of the Cl^- concentration in the assay buffer, while an increase in activity of the mutants under the same conditions is less prominent. For WT PsbO, increasing the Cl^- concentration to 50 mM shifts the pH optimum to 7; although a further increase to 100 mM Cl^- has no effect on the pH optimum, activity is increased to 280 μmol of O_2 (mg of Chl)$^{-1}$ h^{-1}. For PsbO Asp mutants, 50 mM Cl^- shifts the pH optimum to 6.5 while 100 mM Cl^- shifts the optimum to pH 7 and increases maximal activity to 180−200 μmol of O_2 (mg of Chl)$^{-1}$ h^{-1}. The data in Figure 5 show that a high Cl^- concentration (100 mM) eliminates an acidic shift in the pH optimum, which is observed for Asp mutants at low Cl^- concentrations, unifies the pH optimum of all samples at pH 7, but is unable to restore O_2 evolution activity of the mutants to the wild-type level.

DISCUSSION

Structural and Functional Analysis of Asp Mutants. PsbO, as a natively unfolded polypeptide, changes conformation upon binding to PSII by gaining secondary structure at the expense of disordered domains (*5*, *10*, *19*). Figure 6 depicts a three-dimensional homology model of the PSII-bound conformation of wild-type spinach PsbO that was constructed using the crystallographic model of PsbO from the cyanobacterium *T. elongatus* (*8*) as a template. This homology model shows that the PSII-bound conformation of spinach PsbO takes a shape of an extended β-barrel from which the unordered N-terminus and a number of flexible loops protrude. These features resemble those found in the PSII-bound conformation of cyanobacterial PsbO, except that the *T. elongatus* protein has a shorter N-terminus and one additional flexible (cyano) loop in its crystal structure (see refs *8* and *29*). The model of spinach PsbO also reveals that, when bound to PSII, the protein's N-terminus is accessible, while the C-terminus forms a part of the β-barrel with residues buried in the hydrophobic environment. These properties are also present in the PsbO solution structure that has been analyzed in a number of previous biochemical studies (*13*, *15*, *17*, *21*, *23*). The homology model positions Asp157 in the largest flexible loop of the polypeptide (Figure 6). On the basis of the orientation of the amino acid side chains in this model, Asp157 might interact with Arg161 and/or Lys190 (both ~3 Å from Asp157) to facilitate proper folding of the flexible loop during binding of PsbO with PSII intrinsic subunits. The bioinformatics data listed in Table 3 present 23 PsbO sequences of a short domain that is located in the large flexible loop of the protein; this alignment reveals that D157 is fully conserved in both eukaryotes and prokaryotes.

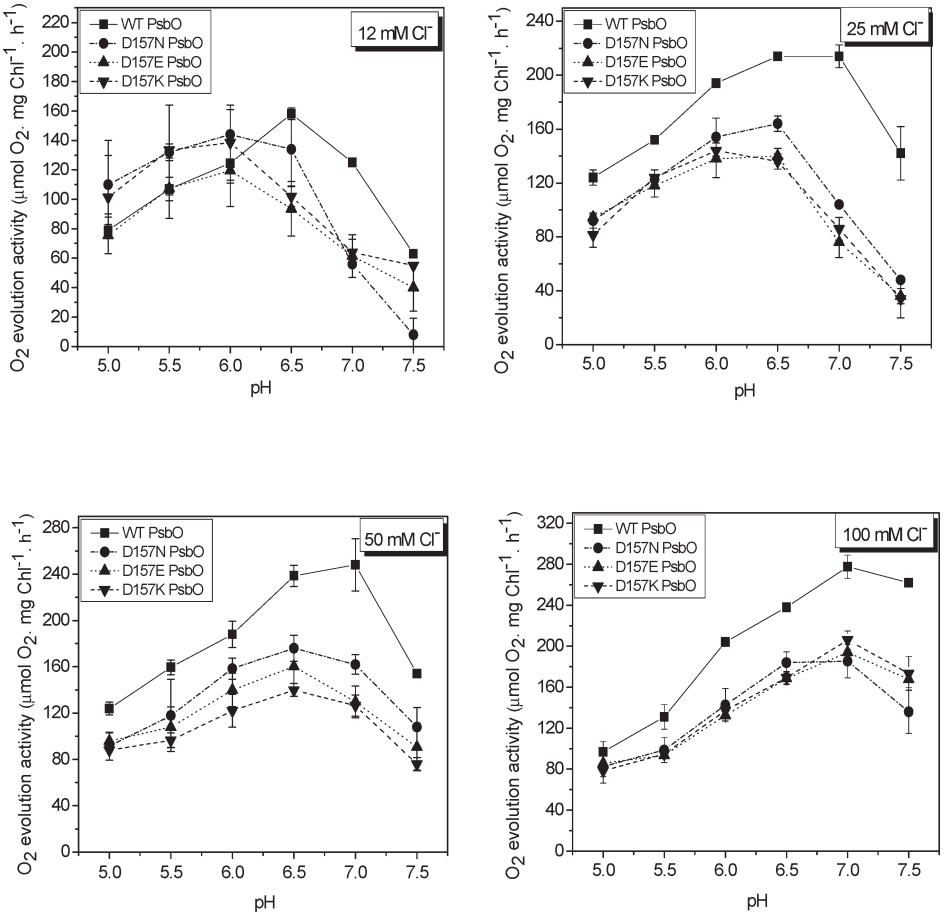

FIGURE 5: O_2 evolution activity of UW-PSII and UW-PSII reconstituted with WT PsbO and Asp157 mutants as a function of pH in assay buffers containing 12, 25, 50, or 100 mM Cl^-. UW-PSII was reconstituted with various PsbO mutants (5 mol of PsbO/mol of PSII) at room temperature for 1 h. Points are the averages, and vertical bars at each point give the standard deviation. The activity of UW-PSII has not been subtracted from the rates shown for WT and the Asp mutants.

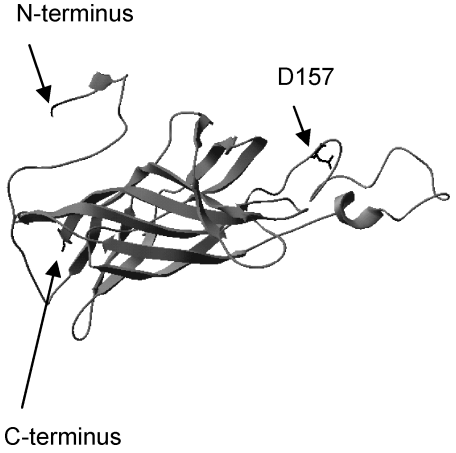

FIGURE 6: Three-dimensional homology model of PsbO (PSII-bound conformation) from spinach, showing the position of Asp157 in the ribbon structure of the protein. A three-dimensional crystallographic model of PSII-bound PsbO from cyanobacterium *T. elongatus* (*8*) was used as the template. Black arrows indicate the flexible and accessible PsbO N-terminus, the Asp157 residue in the large flexible loop of the protein, and the PsbO C-terminus that is buried in the β-sheet barrel.

Spectroscopic analyses of solution tertiary structures of four PsbO species (WT, D157N, D157E, and D157K) revealed a slight modification of the Trp shoulder in the UV absorption spectra of Asp mutants (Figure 4). Spectral characteristics of PsbO Trp241 monitor conformational changes at the PsbO C-terminus (*3*, *17*, *23*), so the slightly less distinct Trp shoulder in the spectra of Asp mutants may indicate a subtle adjustment in the PsbO tertiary structure around the mutants' C-terminus. This adjustment is minor, because the peaks in the near-UV CD spectra (Figure 3) and the size and the secondary structure content (Table 1) of these mutants are similar to those of WT PsbO. Taken together, the spectroscopic analyses presented here suggest that PsbO Asp157 mutants retain a near-wild-type solution structure at 25 °C.

Two copies of PsbO bind per eukaryotic PSII reaction center (*25*, *26*, *38*−*40*); a two-step binding mechanism proposed initial docking of the protein to its PSII binding site(s) through the N-terminus (*21*, *26*, *27*), followed by the functional assembly of PsbO into PSII that activates the enzyme and that requires the intact C-terminus (*23*). The data in Figures 1 and 2 show that the first binding step was not affected by D157 mutagenesis; two copies of PsbO Asp mutants were bound specifically to PSII with an affinity that was similar to that of WT PsbO. All mutants exhibited limited nonspecific binding to PSII when they were used at higher protein concentrations in the reconstitution mixtures. Nonspecific binding was observed previously in other PsbO mutants from spinach (*21*, *26*, *27*) and cyanobacteria (*2*); the cause of the phenomenon is unclear.

Oxygen evolution assays revealed that in spite of their structural and binding properties, Asp157 mutants of PsbO fail to restore more than 30% of the control (SW-PSII) activity

Table 3: Amino Acid Sequence Alignment of the Highly Conserved Domain in the Large Flexible Loop of PsbO[a]

Species	Amino acid sequence
Eukaryotes Spinacia oleracea	FLVPSYRGSS FLDPKGRGGS
Fritillaria agrestis	YLVPSYRGSS FLDPKGRGGS
Bigelowiella natans	FAVPSYRGST FLDPKGRGAA
Nicotiana tabacum	FLVPSYRGSS FLDPKGRGGS
Lycopersicon esculentum	FLVPSYRGSS FLDPKGRGGS
Triticum aestivum	FLVPSYRGSS FLDPKGRGGS
Solanum tuberosum	FLVPSYRGSS FLDPKGRGGS
Pisum sativum	FLVPSYRGSS FLDPKGRGAS
Bruguiera gymnorrhiza	YLVPSYRGSS FLDPKGRGGS
Arabidopsis thaliana	FLVPSYRGSS FLDPKGRGGS
Karenia brevis	FMVPSYRTGL FLDPKGRGTT
Euglena gracilis	FDVPSYRGAT FLDPKGRGGA
Chlamydomonas reinhardtii	FLVPSYRGSS FLDPKGRGGS
Volvox carteri	FVVPSYRGSS FLDPKGRGGS
Heterosigma akashiwo	FTVPSYRTGL FLDPKGRGMS
Isochrysis galbana	FTVPSYRTGL FLDPKGRGTT
Heterocapsa triquetra	FNVPSYRTGG FLDPKGRGMY
Prokaryotes Gloeobacter viol. PCC7421	LVVPSLRGLG YTDSRGRGTD
Synechocystis sp. PCC 6803	FNVPSYRGAG FLDPKARGLY
Thermosynechococcus elong.	FNVPSYRTAN FLDPKGRGLA
Nostoc sp. PCC 7120	FKVPSYRGAA FLDPKGRGVV
Cyanothece sp.	FRVPSYRGAT FLDPKGRGLA
Prochlorococcus marinus	TRTPSYRTSN FLDPKSRALT

[a]The black arrow denotes the D157 residue in the spinach PsbO sequence. Black boxes mark identical amino acid residues, and gray boxes highlight similar residues.

(Figures 1 and 2). These data, in comparison with those previously reported for a number of other PsbO mutants from spinach (*3*, *17*, *20*, *23*, *24*, *28*), show that these Asp mutants are the first genetically modified PsbO species with wild-type PSII binding characteristics that are significantly impaired in terms of O_2 evolution activity. On the basis of this result, we conclude that Asp157 is unnecessary for binding of PsbO to PSII but is a critical residue for PsbO function. This is in contrast to previously published data on the D157N and D157K mutants from spinach PsbO (*41*, *42*) showing decreased PsbO activity for the D157 → N and D157 → K mutations of only 5 and 15%, respectively, compared to that of the wild type. This was interpreted to indicate a lower PSII binding affinity of the mutants rather than a decrease in the level of S-state turnover (*41*, *42*). The PSII preparations used in those experiments had very low activity, and this might have masked the effect of Asp mutations on activity. When a D159N mutation was introduced into *Synechocystis* sp. PCC6803 (D159 in *Synechocystis* sp. PCC6803 is homologous to spinach D157), the mutant exhibited a lower affinity of binding of PsbO to PSII as well as a decrease in O_2 evolution activity (*43*). The analogous mutation, D158N, in *Synechococcus elongatus* significantly affected both activity and binding of the mutant; D158N restored only 18% of wild-type activity, but the amount of PsbO bound to PSII far exceeded that of the wild type, which was interpreted as evidence of substantial nonspecific binding of the mutant. The estimated secondary and tertiary structures of D158N were the same as those for the wild type (*2*), which is similar to the results obtained for the spinach mutants used in this study. In contrast to what was found here for spinach PsbO, the charge-conserving mutation D158E in *S. elongatus* affected neither activity nor PSII binding of the PsbO mutant protein (*2*). The wide-ranging results obtained for PsbO Asp mutants from various organisms (refs *2* and *43* and this study) could be due to differences in the structural organization of PSII in these organisms (*44*), including the fact that only one PsbO subunit per PSII has been found in prokaryotes (*6*−*9*).

Possible Role(*s*) *of PsbO Asp157 in PSII*. It has been proposed that PsbO Asp157 is involved in the putative H^+ channel that links the OEC with the lumen (*6*, *29*). To obtain evidence that low O_2 evolution activity of Asp mutants could be caused by a decline in the proton transfer network, attempts were made to restore the activity of the mutants by chemical rescue using proton acceptors in the assay mixture (data not shown). While the failure to reactivate these samples suggests that Asp157 may not be involved in a proton transfer network, this result must be viewed with caution. Of the reagents used, CCCP is both an efficient proton acceptor and a lipophilic anion that can destabilize $Y_Z^{\bullet}$, the primary donor to $P680^+$ (*45*, *46*). Acetate showed no effect, inhibitory or stimulatory, in our experiments at a concentration of 50 mM, which may reflect the fact that acetate concentrations that are sufficient to cause competitive displacement of Cl^- from the OEC (*47*) had to be avoided in these experiments. As a consequence, it is possible that the elevated Cl^- concentrations used in these experiments would also prevent acetate from reaching a site where it could function as a proton acceptor. We have been unable to discover the origins of

Table 4: K_M Values and Binding Affinities of Various Spinach PsbO Mutants Bound to UW-PSII Preparations

sample	Cl^- K_M	no. of PsbO copies bound per PSII reaction center	activity (% of control)[a]	ref
UW-PSII and WT PsbO	1.0	2 (high affinity)	70	*48*
UW-PSII and R151G PsbO	2.6	2 (low affinity)	20	*28*
UW-PSII and R151D PsbO	2.2	2 (low affinity)	20	*28*
UW-PSII and R161G PsbO	1.6	2 (low affinity)	40	*28*
UW-PSII and ΔT7M PsbO	1.5	1	40	*26*
UW-PSII and ΔS13M PsbO	1.6	1	50	*27*

[a]The 100% control is the O_2 evolution activity of SW-PSII.

inhibition by imidazole, other than to note that the inhibitions were not reversed by increasing concentrations of Cl^- (data not shown).

Nevertheless, the data presented here show that Asp157 has an important role in PsbO function; replacement of Asp157 with another negatively charged residue, Glu, affects PsbO in a manner similar to that of the D → N and D → K mutations (Figure 2). There are several possible explanations. Alterations in the orientation (Glu157) or chemical properties (Asn and Lys) of side chains in the PsbO Asp mutants might affect redox events in the OEC active site and/or prevent a specific interaction that occurs in the wild type between D157 and the PsbO backbone. This interaction may in turn be required to facilitate proper folding of the large flexible loop of the wild-type protein after docking of PsbO to PSII. Conformational flexibility to ensure proper folding of PsbO into PSII appears to be important for activation of the enzyme; an intramolecular cross-link in PsbO prevents reconstitution of O_2 evolution, but not binding of PsbO to PSII or stabilization of the Mn cluster (*44*). The proposal that PsbO D157 affects the redox events in the OEC employs a crystallographic model of PSII from *T. elongatus* that positions PsbO D158 (homologous to D157 in spinach), and few other neighboring PsbO residues, in the proximity of the OEC active site (*8*, *9*). A possible defect in the functional assembly of the mutants into PSII would be reconcilable with our finding that PsbO Asp mutants are less able to retain Cl^- in the OEC than WT PsbO (Table 2 and Figure 5). It is not possible with the available data to determine whether this defect arises from altered transport of Cl^- through an ion channel. Models for channels in the OEC (*9*) near the Cl^- atom detected in the cyanobacterial structure are proposed to be involved in H^+ transport.

Elimination of an acidic shift in the pH optimum for activity when high Cl^- concentrations are added to the assay mixture would be consistent with a competition between Cl^- and OH^- for the PSII binding site, and with the possibility that protection of the Mn cluster by PsbO against OH^- inhibition has been partially compromised by Asp157 mutations. It should also be noted that the coalescence of pH optima in Figure 5 produces a titration curve with an apparent pK_a of ~6.5. This might indicate that a His residue resides in the proton transfer network between the OEC and the lumen and must be deprotonated for oxygen evolution activity to occur. The Asp157 mutants might have affected this residue, but it must reside on one of the intrinsic subunits of PSII; spinach PsbO does not contain His.

It is significant that mutations in Arg151 and Arg161 in PsbO affect Cl^- retention by the OEC and also affect efficient binding of the protein (*28*) and that data on PsbO truncation mutants have also shown that the loss of one of the two bound copies of PsbO affects Cl^- retention (*48*)(Table 4). For all of these mutants, addition of Cl^- in excess of what would be needed to saturate the OEC fails to restore O_2 evolution activity to control levels obtained in PSII reconstituted with WT PsbO. One cause for this would be that inefficient Cl^- retention, caused by subtle structural changes in PsbO, slows the $S_3 \rightarrow S_0$ transition (*49*). It is also possible that PsbO removal or mutation generates changes in PSII electron transfer outside the OEC that cannot be repaired by either Cl^- or rebinding of mutant proteins (*50*). Experiments are underway to examine these possibilities.

ACKNOWLEDGMENT

We thank Nicholas Boswell for assistance with the O_2 evolution assays.

REFERENCES

1. Nelson, N., and Yocum, C. F. (2006) Structure and function of photosystems I and II. *Annu. Rev. Plant Biol. 57*, 521–565.
2. Motoki, A., Usui, M., Shimazu, T., Hirano, M., and Katoh, S. (2002) A domain of the manganese-stabilizing protein from *Synechococcus elongatus* involved in functional binding to Photosystem II. *J. Biol. Chem. 277*, 14747–14756.
3. Popelkova, H., Wyman, A., and Yocum, C. (2003) Amino acid sequences and solution structures of manganese stabilizing protein that affect reconstitution of Photosystem II activity. *Photosynth. Res. 77*, 21–34.
4. Uversky, V. N. (2002) What does it mean to be natively unfolded? *Eur. J. Biochem. 269*, 2–12.
5. Lydakis-Simantiris, N., Hutchison, R. S., Betts, S. D., Barry, B. A., and Yocum, C. F. (1999) Manganese stabilizing protein of photosystem II is a thermostable, natively unfolded polypeptide. *Biochemistry 38*, 404–414.
6. Ferreira, K. N., Iverson, T. M., Maghlaoui, K., Barber, J., and Iwata, S. (2004) Architecture of the photosynthetic oxygen-evolving center. *Science 303*, 1831–1838.
7. Biesiadka, J., Loll, B., Kern, J., Irrgang, K. D., and Zouni, A. (2004) Crystal structure of cyanobacterial photosystem II at 3.2 Å resolution: A closer look at the Mn-cluster. *Phys. Chem. Chem. Phys. 6*, 4733–4736.
8. Loll, B., Kern, J., Saenger, W., Zouni, A., and Biesiadka, J. (2005) Towards complete cofactor arrangement in the 3.0 Å resolution structure of photosystem II. *Nature 438*, 1040–1044.
9. Guskov, A., Kern, J., Gabdulkhakov, A., Broser, M., Zouni, A., and Saenger, W. (2009) Cyanobacterial photosystem II at 2.9 Å resolution and the role of quinones, lipids, channels, and chloride. *Nat. Struct. Mol. Biol. 16*, 334–342.
10. Hutchison, R. S., Betts, S. D., Yocum, C. F., and Barry, B. A. (1998) Conformational changes in the extrinsic manganese stabilizing protein can occur upon binding to the photosystem II reaction center: An isotope editing and FT-IR study. *Biochemistry 37*, 5643–5653.
11. Zubrzycki, I. Z., Frankel, L. K., Russo, P. S., and Bricker, T. M. (1998) Hydrodynamic Studies on the manganese stabilizing protein of photosystem II. *Biochemistry 37*, 13553–13558.
12. Svensson, B., Tiede, D. M., and Barry, B. A. (2002) Small-angle X-ray scattering studies of the manganese stabilizing subunit in Photosystem II. *J. Phys. Chem. B 106*, 8485–8488.
13. Seidler, A. (1994) Introduction of a histidine tail at the N-terminus of the secretory protein expressed in *Escherichia coli*. *Protein Eng. 7*, 1277–1280.
14. Enami, I., Kamo, M., Ohta, H., Takahashi, S., Miura, T., Kusayanagi, M., Tanabe, S., Kamei, A., Motoki, A., Hirano, M., Tomo, T., and

Satoh, K. (1998) Intramolecular cross-linking of the extrinsic 33-kDa protein leads to loss of oxygen evolution but not its ability of binding to photosystem II and stabilization of the manganese cluster. *J. Biol. Chem. 273*, 4629–4634.
15. Shutova, T., Deikus, G., Irrgang, K.-D., Klimov, V. V., and Renger, G. (2001) Origin and properties of fluorescence emission from the extrinsic 33 kDa manganese stabilizing protein of higher plant water oxidizing complex. *Biochim. Biophys. Acta 1504*, 371–378.
16. Tohri, A., Suzuki, T., Okuyama, S., Kamino, K., Motoki, A., Hirano, M., Ohta, H., Shen, J. R., Yamamoto, Y., and Enami, I. (2002) Comparison of the structure of the extrinsic 33 kDa protein from different organisms. *Plant Cell Physiol. 43*, 429–439.
17. Wyman, A. J., Popelkova, H., and Yocum, C. F. (2008) Site-directed mutagenesis of conserved C-terminal Tyrosine and Tryptophan residues of PsbO, the Photosystem II manganese-stabilizing protein, alters its activity and fluorescence properties. *Biochemistry 47*, 6490–6498.
18. Seidler, A., and Michel, H. (1990) Expression in *Escherichia coli* of the *psbO* gene encoding the 33 kDa protein of the oxygen-evolving complex from spinach. *EMBO J. 9*, 1743–1748.
19. Betts, S. D., Ross, J. R., Hall, K. U., Pichersky, E., and Yocum, C. F. (1996) Functional reconstitution of photosystem II with recombinant manganese-stabilizing proteins containing mutations that remove the disulfide bridge. *Biochim. Biophys. Acta 1274*, 135–142.
20. Wyman, A. J., and Yocum, C. F. (2005) Structure and activity of the Photosystem II manganese-stabilizing protein: Role of the conserved disulfide bridge. *Photosynth. Res. 85*, 359–372.
21. Popelkova, H., Im, M. M., D'Auria, J., Betts, S. D., Lydakis-Simantiris, N., and Yocum, C. F. (2002) N-Terminus of the photosystem II manganese stabilizing protein: Effects of sequence elongation and truncation. *Biochemistry 41*, 2702–2711.
22. Betts, S. D., Lydakis-Simantiris, N., Ross, J. R., and Yocum, C. F. (1998) The carboxyl-terminal tripeptide of the manganese-stabilizing protein is required for quantitative assembly into photosystem II and for high rates of oxygen evolution activity. *Biochemistry 37*, 14230–14236.
23. Lydakis-Simantiris, N., Betts, S. D., and Yocum, C. F. (1999) Leucine 245 is a critical residue for folding and function of the manganese stabilizing protein of photosystem II. *Biochemistry 38*, 15528–15535.
24. Betts, S. D., Ross, J. R., Pichersky, E., and Yocum, C. F. (1996) Cold-sensitive assembly of a mutant manganese-stabilizing protein caused by a Val to Ala replacement. *Biochemistry 35*, 6302–6307.
25. Betts, S. D., Ross, J. R., Pichersky, E., and Yocum, C. F. (1997) Mutation Val235Ala weakens binding of the 33-kDa manganese stabilizing protein of Photosystem II to one of two sites. *Biochemistry 36*, 4047–4053.
26. Popelkova, H., Im, M. M., and Yocum, C. F. (2003) Binding of manganese stabilizing protein to photosystem II: Identification of essential N-terminal threonine residues and domains that prevent nonspecific binding. *Biochemistry 42*, 6193–6200.
27. Popelkova, H., Im, M. M., and Yocum, C. F. (2002) N-terminal truncations of manganese stabilizing protein identify two amino acid sequences required for binding of the eukaryotic protein to photosystem II and reveal the absence of one binding-related sequence in cyanobacteria. *Biochemistry 41*, 10038–10045.
28. Popelkova, H., Betts, S. D., Lydakis-Simantiris, N., Im, M. M., Swenson, E., and Yocum, C. F. (2006) Mutagenesis of basic residues R151 and R161 in manganese-stabilizing protein of photosystem II causes inefficient binding of chloride to the oxygen evolving complex. *Biochemistry 45*, 3107–3115.
29. De Las Rivas, J., and Barber, J. (2004) Analysis of the structure of the PsbO protein and its implications. *Photosynth. Res. 81*, 329–343.
30. Hall, T. A. (1999) BioEdit: A user-friendly biological sequence alignment editor and analysis program for Windows 95/98/NT. *Nucleic Acids Symp. Ser. 41*, 95–98.
31. Guex, N., and Peitsch, M. C. (1997) SWISS-MODEL and the Swiss-PdbViewer: An environment for comparative protein modeling. *Electrophoresis 18*, 2714–2723.
32. Schwede, T., Kopp, J., Guex, N., and Peitsch, M. C. (2003) SWISS-MODEL: An automated protein homology-modeling server. *Nucleic Acids Res. 31*, 3381–3385.
33. Arnold, K., Bordoli, L., Kopp, J., and Schwede, T. (2006) The SWISS-MODEL Workspace: A web-based environment for protein structure homology modeling. *Bioinformatics 22*, 195–201.
34. Schmidt, F. X. (1997) Optical Spectroscopy to Characterize Protein Conformation and Conformational Changes. In Protein Structure: A Practical Approach (Creighton, T. E., Ed.) pp 261−297, IRL Pres, New York.
35. Hays, A.-M., Vassiliev, I. R., Golbeck, J. H., and Debus, R. J. (1998) Role of D1-His190 in proton coupled electron transfer reaction in PhotosystemII: A chemical complementation study. *Biochemistry 37*, 11352–11365.
36. Guan, Y., Zhang, W., Deng, M., Jin, M., and Yu, X. (2004) Significant enhancement of photobiological H_2 evolution by carbonylcyanide *m*-chlorophenylhydrazone in the marine green algae *Platymonas subcordiformis*. *Biotechnol. Lett. 26*, 1031–1035.
37. Takahashi, E., and Wraight, C. A. (2006) Small weak acids reactivate proton transfer in reaction centers from *Rhodobacter sphaeroides* mutated at Asp^{L210} and Asp^{M17}. *J. Biol. Chem. 281*, 4413–4422.
38. Xu, Q., and Bricker, T. M. (1992) Structural organization of proteins on the oxidizing side of photosystem II: 2 Molecules of the 33-kDa manganese-stabilizing proteins per reaction center. *J. Biol. Chem. 267*, 25816–25821.
39. Leuschner, C., and Bricker, T. M. (1996) Interaction of the 33 kDa extrinsic protein with photosystem II: Rebinding of the 33 kDa extrinsic protein to photosystem II membranes which contain four, two, or zero manganese per photosystem II reaction center. *Biochemistry 35*, 4551–4557.
40. Murakami, R., Ifuku, K., Takabayashi, A., Shikanai, T., Endo, T., and Sato, F. (2005) Functional dissection of two *Arabidopsis* PsbO proteins. *FEBS J. 272*, 2165–2175.
41. Seidler, A., Roll, K., and Michel, H. (1992) Characterization of the 33 kDa protein of the oxygen-evolving complex of higher plants by site-directed mutagenesis. In Research in Photosynthesis (Murata, N., Ed.) Vol. II, pp 409−413, Kluwer Academic Publishers, Dordrecht, The Netherlands.
42. Seidler, A., Michel, H., and Rutherford, A. W. (1996) The extrinsic 33 kDa protein of photosystem II: Improved expression plasmids and progress in the mutational analysis. In Photosynthesis: From Light to Biosphere (Mathis, P., Ed.) Vol. II, pp 259−262, Kluwer Academic Publishers, Dordrecht, The Netherlands.
43. Burnap, R. L., Qian, M., Shen, J. R., Inoue, Y., and Sherman, L. A. (1994) Role of disulfide linkage and putative intermolecular binding residues in the stability and binding of the extrinsic manganese-stabilizing protein to the photosystem II reaction-center. *Biochemistry 33*, 13712–13718.
44. Enami, I., Okumura, A., Nagao, R., Suzuki, T., Iwai, M., and Shen, J.-R. (2008) Structure and function of the extrinsic proteins of photosystem II from different species. *Photosynth. Res. 98*, 349–363.
45. Renger, G. (1969) Reaction of CCCP in photosynthesis on an intermediate between chlorophyll a_{II} and water. *Naturwissenschaftern 56*, 370.
46. Ghanotakis, D. F., Yerkes, C. T., and Babcock, G. T. (1982) The role of reagents accelerating the deactivation reactions of water-spitting enzyme system Y (ADRY reagents) in destabilizing high-potential oxidizing equivalents generated in chloroplast photosystem II. *Biochim. Biophys. Acta 682*, 21–31.
47. Sandusky, P. O., and Yocum, C. F. (1988) The chloride requirement for photosynthetic oxygen evolution: Factors affecting nucleophilic displacement of chloride from the oxygen-evolving complex. *Biochim. Biophys. Acta 849*, 85–93.
48. Popelkova, H., Commet, A., Kuntzleman, T., and Yocum, C. F. (2008) Inorganic cofactor stabilization and retention: The unique functions of the two PsbO subunits of eukaryotic Photosystem II. *Biochemistry 47*, 12953–12600.
49. Wincencjusz, H., Gorkom, H. J., and Yocum, C. F. (1997) The photosysnthetic oxygen evolution complex requires chloride for its redox state $S_2 \rightarrow S_3$ and $S_3 \rightarrow S_0$ transitions but not for $S_0 \rightarrow S_1$ or $S_1 \rightarrow S_2$ transitions. *Biochemistry 36*, 3663–3670.
50. Andreasson, L.-E., Vass, I., and Styring, S. (1995) Ca^{2+} depletion modifies the electron transfer on both donor and acceptor sides in photosystem II from spinach. *Biochim. Biophys. Acta 1230*, 155–164.
51. Sreerama, N., and Woody, R. W. (2000) Estimation of protein secondary structure from circular dichroism spectra: Comparison of CONTIN, SELCON and CDSSTR methods with an expanded reference set. *Anal. Biochem. 287*, 252–260.